Adaptive Sparsified Graph Learning Framework for Vessel Behavior Anomalies

Jeehong Kim^{1*}, Minchan Kim^{1*}, Jaeseong Ju¹, Youngseok Hwang¹, Wonhee Lee², Hyunwoo Park^{1†}

¹Graduate School of Data Science, Seoul National University ²Korea Research Institute of Ships and Ocean Engineering {williamkim10, mmm5373, hyunwoopark}@snu.ac.kr

Abstract

Graph neural networks have emerged as a powerful tool for learning spatiotemporal interactions. However, conventional approaches often rely on predefined graphs, which may obscure the precise relationships being modeled. Additionally, existing methods typically define nodes based on fixed spatial locations, a strategy that is ill-suited for dynamic environments like maritime environments. Our method introduces an innovative graph representation where timestamps are modeled as distinct nodes, allowing temporal dependencies to be explicitly captured through graph edges. This setup is extended to construct a multi-ship graph that effectively captures spatial interactions while preserving graph sparsity. The graph is processed using Graph Convolutional Network layers to capture spatiotemporal patterns, with a forecasting layer for feature prediction and a Variational Graph Autoencoder for reconstruction, enabling robust anomaly detection.

Introduction

Graph neural network (GNN) based methods provided a powerful approach for modeling spatiotemporal data (Yu, Yin, and Zhu 2017), yet existing approaches often relied on predefined or fully connected graphs (Liu et al. 2023; Zhang et al. 2023), introducing noise and reducing interpretability. Additionally, most graph based anomaly detection methods primarily utilized graphs for node embedding updates, rather than fully utilizing their structural and relational properties (Liu et al. 2023; Zhang et al. 2023).

We introduce a novel framework for anomaly detection in multi-ship trajectory data by utilizing a sparsified graph, removing noisy and task-irrelevant edges while retaining essential spatiotemporal relationships. The optimized graph is then embedded using Graph Convolutional Network (GCN) (Kipf and Welling 2016a) layers to effectively capture these relationships. Furthermore, leveraging a Variational Graph Autoencoder (VGAE) (Kipf and Welling 2016b), our framework reconstructs adjacency matrices, allowing anomaly detection by identifying discrepancies in graph structures.

Our contributions are summarized as follows:

Copyright © 2025, Association for the Advancement of Artificial Intelligence (www.aaai.org). All rights reserved.

- Novel Graph Representation: We establish a graph-based input structure for moving objects, representing each timestamp as a node to explicitly model temporal dependencies through graph edges.
- Efficient Graph Construction Strategy: We generate a multi-ship graph that effectively captures spatial relationships while preserving graph sparsity.
- Graph Based Anomaly Detection: Our framework combines prediction and reconstruction within a graph based approach, fully leveraging graph structures to enhance anomaly detection performance.

Related Works

Spatiotemporal GNNs Existing spatiotemporal methods often relied on fixed spatial locations, such as intersections (Wang et al. 2020; Yu, Yin, and Zhu 2017), which were unsuitable for the dynamic and fluid nature of maritime environments. Consequently, although efforts were made to establish dynamic reference points that were appropriate for the maritime domain (Eljabu, Etemad, and Matwin 2021; Liang et al. 2022), these points still did not adequately capture the fluid and constantly evolving nature of moving vessels.

Vessel Behavior Anomaly The concept of anomalies in AIS tracks refers to behaviors that deviate from what is considered 'normal' or expected under typical operational conditions (Laxhammar 2008). There are many studies (Lane et al. 2010; Davenport 2008; Liu, Li, and Liu 2024) that define anomalous behaviors based on kinematic behaviors, AIS transmission behaviors, and other supplementary behaviors that occur on the ship. One of the key challenges in defining anomalies is the absence of a universal criterion for what constitutes an anomalous event. Despite the wide range of possible anomalies, this study specifically focuses on deviation from standard route. This type of anomaly is one of the most fundamental and frequently observed irregularities in vessel movement, serving as a crucial indicator of potential maritime risks. A vessel straying from its expected trajectory could signal various underlying causes, including adverse weather conditions, mechanical failures, unauthorized maneuvers, or illicit activities. By analyzing deviations from standard routes, we aim to establish a robust framework for

^{*}These authors contributed equally.

[†]Corresponding author

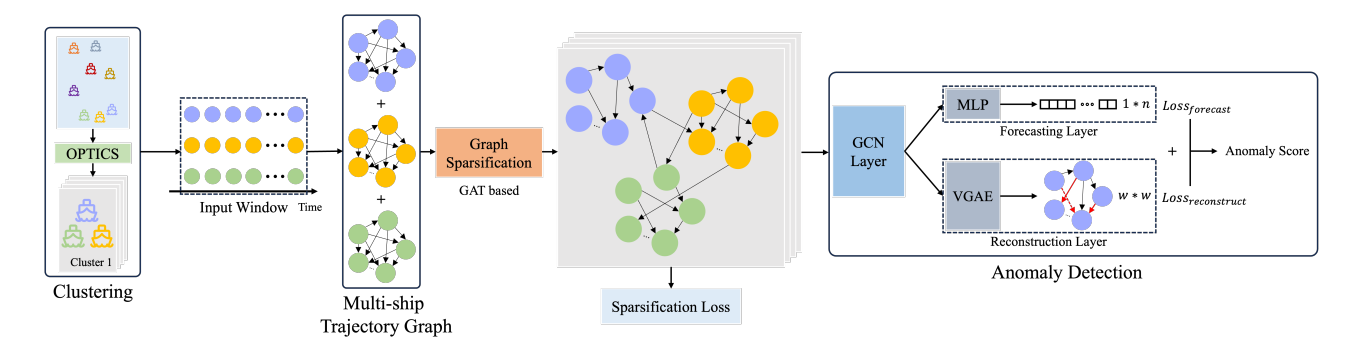


Figure 1: Our framework employs a multi-component architecture designed to learn a sparsified graph structure. The learned graph is then embedded using GCN layers, which supports both the forecasting and reconstruction processes. The combined loss from these components is utilized for effective anomaly detection.

detecting navigational anomalies in real-world maritime operations. The rationale behind this selection will be elaborated more in the experimental section, where we detail the statistical techniques used to quantify deviations.

GNN Based Vessel Anomaly Detection The objective of vessel anomaly detection is to identify unusual movement patterns, which are often caused by mechanical failures or navigational errors (Ribeiro, Paes, and de Oliveira 2023). Most existing methods constructed graphs using predefined or fully connected structures (Jiang et al. 2024; Liu et al. 2023; Wolsing et al. 2022; Zhang et al. 2023). Nevertheless, these methodologies proved inadequate for capturing meaningful spatiotemporal relationships that are well-suited to the task at hand.

Methodology

Problem Definition

Given AIS data $\mathcal{X} = \{\mathbf{x}_i^t | i \in \mathcal{V}_t, t \in T\}$, where \mathbf{x}_i^t represents the feature vector of ship i at time t, and a series of temporal graphs $\{\mathcal{G}_t\}_{t=1}^T$, the objective is to:

- 1. Predict the *next time step embedding* \mathbf{h}_i^{t+1} for each node $i \in \mathcal{V}_t$ using past observations and graph structure.
- 2. Identify anomalous nodes and edges in \mathcal{G}_{w_t} by comparing observed patterns to learned normal behavior.

The proposed approach combines *node embedding, graph* sparsification, time-series forecasting, and anomaly detection into a unified framework to effectively handle these challenges.

As depicted in Figure 1, our paper establishes a novel framework for vessel anomaly detection leveraging graph neural networks to model multi-ship trajectory data.

Graph Construction

To define the boundaries of multi-ship graphs, the OPTICS clustering algorithm (Ankerst et al. 1999) is employed. This algorithm groups ships based on the latitude and longitude at a given time stamp t, thereby identifying clusters that reflect shared spatiotemporal regions.

Algorithm 1: Graph Initialization

Input: Timestamps of ship i: $t_1^i, t_2^i, \ldots, t_n^i$, window size w **Output**: Graphs $\mathcal{G}_{w_1}^i, \mathcal{G}_{w_2}^i, \ldots, \mathcal{G}_{w_m}^i$

- 1: **for** each sliding window w_k **do**
- 2: Initialize graph $\mathcal{G}_{w_k}^i = (\mathcal{V}_{w_k}^i, \mathcal{E}_{w_k}^i)$
- 3: $\mathcal{V}_{w_k}^i \leftarrow \text{timestamps in } w_k$
- 4: **for** each pair of timestamps (t_1, t_2) where $t_1, t_2 \in w_k$ and $t_1 < t_2$ **do**
- 5: Add directed edge $e_{t_1 \to t_2}$ to $\mathcal{E}_{w_k}^i$
- 6: **end for**
- 7: end for
- 8: return $\mathcal{G}_{w_1}^i, \mathcal{G}_{w_2}^i, \dots, \mathcal{G}_{w_m}^i$

Graph Initialization Unlike conventional GNN tasks where the initial graph structure is predefined, our approach starts by constructing the graph from raw data. In our case, the graph is constructed within each identified cluster from the previous step. The core idea is illustrated on lines 4–5 of Algorithm 1, where each edge represents a temporal connection between consecutive timestamps.

The underlying intuition behind this approach is to demonstrate that, rather than relying on traditional time-series prediction models such as RNN (Rumelhart, Hinton, and Williams 1986) or LSTM (Hochreiter 1997), temporal dependencies can be effectively captured within a graph structure. By embedding sequential relationships as edges in the graph, we establish a framework where time-series forecasting can be performed using a simple MLP model. This highlights the feasibility of leveraging graph-based representations for temporal modeling, enabling efficient and scalable predictions without the need for complex recurrent architectures.

Multi-ship Trajectory Graph Then the multi-ship trajectory graph is constructed in the same context for a single ship while only considering the ships within the same cluster. This guarantees that the graph encompasses both intraship and inter-ship temporal interactions.

Algorithm 2: Graph Sparsification

Input: Graph $\mathcal{G}^i = (\mathcal{V}^i, \mathcal{E}^i)$ Output: Sparsified Graph $\mathcal{G}^i_{\text{sparse}}$

- 1: Initialize sparsification function F
- 2: Apply F to \mathcal{G}_i :

$$\mathcal{G}_i^{\text{sparse}} = F(\mathcal{G}_i)$$

- 3: Perform downstream tasks using $\mathcal{G}_{ ext{sparse}}^i$
- 4: Compute L_{forecast} and $L_{\text{reconstruct}}$
- 5: Apply sparsity regularization with L_0 norm:

$$L_{\text{total}} = L_{\text{forecast}} + L_{\text{reconstruct}} + \lambda ||Z||_{0}$$

- 6: Optimize $\mathcal{G}_{\text{sparse}}^i$ by minimizing L_{total}
- 7: **return** $\mathcal{G}_{\text{sparse}}^{i}$

Graph Sparsification

Graph sparsification is essential for efficient computation, particularly when the graph is initially constructed using Algorithm 1. Algorithm 2 focuses on learning an edge-sparsified graph by systematically removing noisy and task-irrelevant edges. It is based on SGAT (Ye and Ji 2021), which employs a binary mask $Z \in \{0,1\}^M$, where M denotes the total number of edges. The function of the mask z_{ij} is to determine whether the edge e_{ij} is used during neighbor aggregation. The adjacency matrix A is modified as $\bar{A} = A \odot Z$ and sparsification is achieved by optimizing a regularized loss of the L_0 norm.

While there is a separate regularization for this process, recent approaches (Li et al. 2024) suggest integrating the term directly with the downstream task loss, which could offer a more unified optimization framework. Further advancements in this direction can be explored through the emerging field of *Graph Structural Learning*, which has gained significant attention in recent research.

Anomaly Detection

The anomaly detection process begins with the sparsified graph derived from the multi-ship trajectory graph, which is then subjected to a series of GCN layers. These layers capture structural and spatiotemporal patterns, embedding them into node representations.

The output of the GCN layers is proceeded to two additional layers, namely the *forecasting layer* and the *reconstruction layer*. These stages are performed at the individual ship level for a tailored process, where each ship's trajectory is treated as an independent subgraph.

The two-layer design integrates both forecasting and reconstructive perspectives, enabling comprehensive anomaly detection for temporal deviations and feature distortions. By leveraging the graph's inductive bias, specifically the directed edges that are constructed upon temporal dependencies, the architecture eliminates the need for sequential models like LSTM or GRU, ensuring a streamlined and robust design for diverse graph structures.

$$L_{\text{total}} = L_{\text{forecast}} + L_{\text{reconstruct}} + \lambda ||Z||_{0}$$
 (1)

Forecasting The forecasting layer employs a simple multi-layer perceptron (MLP) to predict the feature values at the subsequent time step for each node, utilizing the temporal dependencies encoded by the GCN layers. A discrepancy between the predicted and actual values may be indicative of a potential anomaly.

Reconstruction The reconstruction layer utilizes VGAE to process individual ship trajectories as distinct subgraphs, encoding their structural and feature information into a compact latent space. The VGAE reconstructs the adjacency matrix, with anomalies identified based on reconstruction errors derived from the differences between the original and reconstructed subgraph properties. By capturing subgraph level patterns, this approach facilitates robust anomaly detection for individual ship trajectories.

$$L_{\text{reconstruct}} = \mathbb{E}_{q(Z|X,\bar{A})}[\log p(\bar{A}, X|Z)] -\beta \cdot D_{\text{KL}}(q(Z|X, \bar{A}) || p(Z))$$
(2)

Anomaly Scoring To detect anomalous data points, we adopt a reasoning score that integrates both the prediction error and the node reconstruction probability (Liu et al. 2023). For each data point i, the reasoning score is defined as

$$RS_i = \frac{E_i + \gamma \cdot (1 - P_i)}{1 + \gamma},\tag{3}$$

where E_i denotes the mean squared error between predicted and actual values, P_i is the node reconstruction probability representing the likelihood of observing the feature values under the learned model, and γ is a hyperparameter that controls the balance between these two components. The optimal value of γ can be determined through validation on the training set.

To determine the anomaly threshold, we employ the Peak-Over-Threshold (POT) method, which dynamically adjusts the threshold based on environmental changes. This approach classifies a data point as anomalous when its prediction and reconstruction errors exceed the dynamically set threshold, allowing for more adaptive and robust anomaly detection in varying maritime conditions.

Experiment

Dataset

In this paper, we use the *OMTAD dataset* (Masek et al. 2021), which was constructed from the Australian Maritime Safety Authority (AMSA), using anonymized AIS data. We specifically focused on the Western Australian waters due to its high vessel traffic density, as it represents one of the busiest maritime routes in the region. Figure 2 shows the visualization of vessel trajectories in this area. The dataset contains fundamental AIS features: longitude, latitude, Speed over Ground (SOG), and Course over Ground (COG), with data points sampled at one-hour intervals. Vessel journeys were segmented based on stoppage (zero speed) or data gaps (>3.5 hours), and only tracks at least 10 hours long were retained. Missing data was interpolated using linear interpolation, with manual verification ensuring data quality. The fi-



Figure 2: Visualization of maritime vessel trajectories from the OMTAD dataset in Western Australian waters, one of the most congested maritime areas in the region. The movement paths show vessel positions over a 5-hour period, with lines representing trajectories and points indicating vessel positions. The OPTICS algorithm identified distinct vessel clusters (shown in different colors), while gray trajectories represent non-clustered vessels classified as noise.

nal dataset includes 19,124 vessel tracks, categorized by vessel type (cargo, tanker, passenger), year, and month. While the original dataset included fishing vessels as a fourth category, we excluded them from our analysis as their distinctive movement patterns significantly differ from the other vessel types and could potentially be misclassified as anomalies in our model.

Synthetic Anomaly Generation A major challenge in maritime anomaly detection is the lack of ground truth labels. In cases where labeled anomalies exist, they are typically annotated by domain experts, which is impractical for large-scale datasets. To address this issue, many existing approaches synthesize anomalies by injecting artificial perturbations into normal data. Inspired by this, we generate synthetic anomalies based on the Speed and Course Anomaly (SCA) defined by (Liu, Li, and Liu 2024). SCA is characterized by abnormal changes in both speed and course, making it one of the most commonly observed anomalies in vessel trajectories.

To synthesize such anomalies, we model the statistical properties of normal vessel movements and introduce perturbations in the SOG and COG values. Specifically, we assume that the rate of change in SOG and COG follows a normal distribution:

$$a \sim \mathcal{N}(\mu_a, \sigma_a^2), \quad \omega \sim \mathcal{N}(\mu_\omega, \sigma_\omega^2)$$
 (4)

 $a \sim \mathcal{N}(\mu_a, \sigma_a^2), \quad \omega \sim \mathcal{N}(\mu_\omega, \sigma_\omega^2) \tag{4}$ where $a_i = \frac{SOG_i - SOG_{i-1}}{\Delta t}$ and $\omega_i = \frac{COG_i - COG_{i-1}}{\Delta t}$ denote the change rate of speed and course, respectively. Here, i represents the index of a data point in the trajectory, and Δt is the time interval between consecutive AIS messages.

To introduce synthetic anomalies, we perturb the speed and course change rates by sampling values that significantly deviate from their normal distribution:

$$a_i^* = \mu_a + k \cdot \sigma_a, \quad \omega_i^* = \mu_\omega + k \cdot \sigma_\omega$$
 (5)

where k is a scaling factor that determines the severity of the anomaly. A typical choice is k > 3, ensuring that the new values fall outside the normal range (beyond the 99.7% confidence interval).

Once the synthetic anomaly values a_i^* and ω_i^* are generated, the corresponding speed and course values are updated iteratively:

$$SOG_i^* = SOG_{i-1} + a_i^* \cdot \Delta t \tag{6}$$

$$COG_i^* = COG_{i-1} + \omega_i^* \cdot \Delta t \tag{7}$$

where SOG_i^* and COG_i^* represent the modified speed and course values containing synthetic anomalies.

This process is applied to randomly selected trajectory points, ensuring that a subset of the dataset contains anomalous behavior. The generated anomalies effectively simulate real-world vessel irregularities, such as sudden acceleration, deceleration, or unexpected course deviations, making them valuable for training and evaluating anomaly detection mod-

Experimental Setup

All experiments were implemented using PyTorch 2.0 and PyTorch Geometric frameworks. Our architecture consists of a GCN encoder with 64 hidden channels and 32 latent dimensions, utilizing LayerNorm for stable training. For graph construction, we employed a sliding window approach with h=10 hours and 1-hour steps. Each node encodes a vessel state through five features: geographical coordinates, speed, and course decomposed into sine and cosine components. This decomposition of course angle was necessary to preserve the circular nature of angular data, as direct use of raw angles would create discontinuity at the 0/360-degree boundary.

The model was trained using the Adam optimizer with a learning rate of 0.001 and weight decay of 1e-5. We trained for a maximum of 100 epochs with early stopping (patience=10) to prevent overfitting. The loss function combines three components: forecasting loss (MSE), graph reconstruction loss, and KL divergence term. For synthetic anomaly generation, we set track_anomaly_ratio=0.1 (10\%) of tracks contain anomalies) and point_anomaly_ratio=0.3 (30% of points within anomalous tracks), with severity factor k = 3.5.

The dataset was partitioned to ensure all synthetic anomalies appeared exclusively in the test set to maintain uncontaminated training data. Specifically, any trajectory containing y = 0 values was allocated to the test set, while the remaining data was split into training (90%) and validation (10%) sets. Input features were normalized using per-graph standardization to ensure stable training.

Conclusion and Future Work

The proposed framework will be validated using AIS data, with comparative analyses conducted alongside existing anomaly detection models to evaluate performance. Furthermore, efforts will be made to refine the methodology through the use of adaptive graph construction techniques, with the aim of assessing its robustness and scalability across various maritime scenarios.

References

Ankerst, M.; Breunig, M. M.; Kriegel, H.-P.; and Sander, J. 1999. OPTICS: Ordering points to identify the clustering structure. *ACM Sigmod record*, 28(2): 49–60.

Davenport, M. 2008. Kinematic behaviour anomaly detection (KBAD)-Final report. *DRDC CORA report KBAD-RP-52-6615*.

Eljabu, L.; Etemad, M.; and Matwin, S. 2021. Anomaly detection in maritime domain based on spatio-temporal analysis of ais data using graph neural networks. In 2021 5th International Conference on Vision, Image and Signal Processing (ICVISP), 142–147. IEEE.

Hochreiter, S. 1997. Long Short-term Memory. *Neural Computation MIT-Press*.

Jiang, J.; Zuo, Y.; Xiao, Y.; Zhang, W.; and Li, T. 2024. STMGF-Net: A Spatiotemporal Multi-Graph Fusion Network for Vessel Trajectory Forecasting in Intelligent Maritime Navigation. *IEEE Transactions on Intelligent Transportation Systems*.

Kipf, T. N.; and Welling, M. 2016a. Semi-supervised classification with graph convolutional networks. *arXiv* preprint *arXiv*:1609.02907.

Kipf, T. N.; and Welling, M. 2016b. Variational graph autoencoders. *arXiv preprint arXiv:1611.07308*.

Lane, R. O.; Nevell, D. A.; Hayward, S. D.; and Beaney, T. W. 2010. Maritime anomaly detection and threat assessment. In 2010 13th International conference on information fusion, 1–8. IEEE.

Laxhammar, R. 2008. Anomaly detection for sea surveillance. In 2008 11th international conference on information fusion, 1–8. IEEE.

Li, Z.; Sun, X.; Luo, Y.; Zhu, Y.; Chen, D.; Luo, Y.; Zhou, X.; Liu, Q.; Wu, S.; Wang, L.; et al. 2024. GSLB: the graph structure learning benchmark. *Advances in Neural Information Processing Systems*, 36.

Liang, M.; Liu, R. W.; Zhan, Y.; Li, H.; Zhu, F.; and Wang, F.-Y. 2022. Fine-grained vessel traffic flow prediction with a spatio-temporal multigraph convolutional network. *IEEE Transactions on Intelligent Transportation Systems*, 23(12): 23694–23707.

Liu, H.; Jia, Z.; Li, B.; Liu, Y.; and Qi, Z. 2023. The model of vessel trajectory abnormal behavior detection based on graph attention prediction and reconstruction network. *Ocean Engineering*, 290: 116316.

Liu, J.; Li, J.; and Liu, C. 2024. AIS-based kinematic anomaly classification for maritime surveillance. *Ocean Engineering*, 305: 118026.

Masek, M.; Lam, C. P.; Rybicki, T.; Snell, J.; Wheat, D.; Kelly, L.; Smith-Gander, C.; et al. 2021. The open maritime traffic analysis dataset.

Ribeiro, C. V.; Paes, A.; and de Oliveira, D. 2023. AIS-based maritime anomaly traffic detection: A review. *Expert Systems with Applications*, 231: 120561.

Rumelhart, D. E.; Hinton, G. E.; and Williams, R. J. 1986. Learning representations by back-propagating errors. *nature*, 323(6088): 533–536.

Wang, X.; Ma, Y.; Wang, Y.; Jin, W.; Wang, X.; Tang, J.; Jia, C.; and Yu, J. 2020. Traffic flow prediction via spatial temporal graph neural network. In *Proceedings of the web conference* 2020, 1082–1092.

Wolsing, K.; Roepert, L.; Bauer, J.; and Wehrle, K. 2022. Anomaly detection in maritime AIS tracks: A review of recent approaches. *Journal of Marine Science and Engineering*, 10(1): 112.

Ye, Y.; and Ji, S. 2021. Sparse graph attention networks. *IEEE Transactions on Knowledge and Data Engineering*, 35(1): 905–916.

Yu, B.; Yin, H.; and Zhu, Z. 2017. Spatio-temporal graph convolutional networks: A deep learning framework for traffic forecasting. *arXiv preprint arXiv:1709.04875*.

Zhang, Y.; Jin, Q.; Liang, M.; Ma, R.; and Liu, R. W. 2023. Vessel Behavior Anomaly Detection Using Graph Attention Network. In *International Conference on Neural Information Processing*, 291–304. Springer.

Appendix

Bounded Position Change Under Small Perturbations in SOG and COG A key assumption in the anomaly generation process is that modifying SOG and COG does not significantly alter the vessel's position. The following theorem provides a theoretical justification for this assumption.

Theorem 1. For a sufficiently small perturbation ϵ , if the SOG and COG satisfy the following conditions:

$$|a_i^*| \le \epsilon SOG_{i-1}, \quad |\omega_i^*| \le \epsilon COG_{i-1}$$

then the resulting position change remains bounded by:

$$|\Delta \phi^*| \le \epsilon \Delta t, \quad |\Delta \lambda^*| \le \epsilon \Delta t$$

implying that the vessel remains effectively on the same trajectory. where

• $\Delta\phi^*$ and $\Delta\lambda^*$ denote the changes in latitude and longitude, respectively.

Theorem 1 ensures that, under controlled perturbations, the trajectory remains unchanged, making it valid to generate anomalies by modifying only SOG and COG. Further proof is provided in the Appendix section.

Proof of Theorem 1 We start by defining the changes in latitude and longitude. Let R denote the Earth's radius. The latitude change $\Delta\phi^*$ is computed using R, while the longitude change $\Delta\lambda^*$ is adjusted by $R\cos\phi$ to account for the varying circumference of the Earth at different latitudes:

$$\Delta \phi^* = \frac{SOG_i^* \cos(COG_i^*)}{R} \cdot \Delta t$$

$$\Delta \lambda^* = \frac{SOG_i^* \sin(COG_i^*)}{R \cos \phi} \cdot \Delta t$$

Substituting the perturbed values of SOG and COG, we obtain:

$$\Delta \phi^* = \frac{(SOG_{i-1} + a_i^* \cdot \Delta t) \cos(COG_{i-1} + \omega_i^* \cdot \Delta t)}{R} \cdot \Delta t$$

$$\Delta \lambda^* = \frac{(SOG_{i-1} + a_i^* \cdot \Delta t) \sin(COG_{i-1} + \omega_i^* \cdot \Delta t)}{R\cos\phi} \cdot \Delta t$$

Using the Taylor series expansion for small x, we approximate:

$$\cos(COG_i^*) \approx \cos(COG_{i-1}) - \sin(COG_{i-1}) \cdot \omega_i^* \cdot \Delta t$$

$$\sin(COG_i^*) \approx \sin(COG_{i-1}) + \cos(COG_{i-1}) \cdot \omega_i^* \cdot \Delta t$$

By substituting these approximations back into the expressions for $\Delta \phi^*$ and $\Delta \lambda^*$, we get:

$$\Delta \phi^* \approx \frac{SOG_{i-1} \left(1 + \frac{a_i^*}{SOG_{i-1}} \right) \cos COG_{i-1}}{R} \cdot \Delta t$$

$$\Delta \lambda^* \approx \frac{SOG_{i-1} \left(1 + \frac{a_i^*}{SOG_{i-1}}\right) \sin COG_{i-1}}{R\cos \phi} \cdot \Delta t$$

Since we assume:

$$|a_i^*| \le \epsilon SOG_{i-1}, \quad |\omega_i^*| \le \epsilon COG_{i-1}$$

it follows that:

$$|\Delta \phi^*| \le \epsilon \Delta t, \quad |\Delta \lambda^*| \le \epsilon \Delta t$$

which ensures that for a sufficiently small ϵ , the vessel remains effectively on the same trajectory.